LA-10525-MS

Los Alamos National Laboratory is operated by the University of California for the United States Department of Energy under contract W-7405-ENG-36.

[illegible]ted-Particle Production in a Sphere [illegible]D Irradiated by 14-MeV Neutrons

Los Alamos
Los Alamos National Laboratory
Los Alamos, New Mexico 87545

LA-10525-MS

UC-34C
Issued: November 1985

Charged-Particle Production in a Sphere of ^{6}LiD Irradiated by 14-MeV Neutrons

Leona Stewart*
L. Raymond Fawcett, Jr.**
Gary D. Doolen
Robert C. Little

*Consultant at Los Alamos.
**Collaborator at Los Alamos. Director of Physics and Pre-Engineering Programs, Longwood College, Farmville, VA 23901.

Los Alamos National Laboratory
Los Alamos, New Mexico 87545

CONTENTS

CHARGED-PARTICLE PRODUCTION IN A SPHERE OF ^{6}LiD IRRADIATED BY 14-MeV NEUTRONS

by

Leona Stewart, L. Raymond Fawcett, Jr., Gary D. Doolen, and Robert C. Little

ABSTRACT

The production of protons, deuterons, tritons, and alpha particles in a sphere of ^{6}LiD irradiated by a central source of 14-MeV neutrons has been investigated. The Los Alamos Monte Carlo Neutron Photon (MCNP) transport code was used to calculate neutron transport through—and charged-particle production in—the ^{6}LiD sphere. The numbers of charged-particles produced were compared with those predicted by a diffusion code that also transported the charged particles. The tritium production was also compared with the experiment. It was found that charged-particle generation from 14-MeV neutrons on ^{6}LiD is prolific.

I. INTRODUCTION

In 1976, Hemmendinger et al.[1] measured the tritium produced when ampules containing ^{6}LiH and ^{7}LiH were embedded at various positions in a 30-cm radius sphere of ^{6}LiD.* A 14-MeV source placed at the center of the sphere produced $9.42 \pm 0.28 \times 10^{15}$ neutrons. In addition to the ampules of lithium hydride, radiochemical foils of ^{45}Sc, ^{89}Y, ^{90}Zr, ^{169}Tm, ^{191}Ir, ^{193}Ir, ^{197}Au, ^{235}U, and ^{238}U were used to monitor the neutron flux as a function of penetration depth in the sphere. In the analysis of the experiment,[1] all the neutrons are assumed to come from the source or from neutron interactions with deuterium or lithium in the sphere. It is well known, however, that ions are produced from neutrons elastically scattered from deuterium and lithium and that the interaction cross sections for the production of high-energy charged particles are large at all neutron energies. Furthermore, these charged particles could, in turn, produce other neutrons. These neutrons are assumed to have negligible effect upon the measured and calculated spectral and flux distributions. It seemed appropriate to investigate this assumption.

As a first step, the number of charged particles produced at 12 positions along the radius of the ^{6}LiD sphere was calculated with the Monte Carlo Neutron Photon (MCNP) transport code.[2] The neutron spectra were also calculated at these radial positions, and in a separate MCNP run, the neutron currents were tallied. The charged particles tabulated were protons, deuterons, tritons, and alpha particles. (^{3}He particles are not produced from neutron interactions with deuterium or ^{6}Li).

Because of interest in using helium detectors to determine reaction rates and absolute fluxes, a second calculation was performed with a diffusion code (quite different from MCNP) to determine the charged-particle production. Agreement to approximately 10-15% was observed for protons, tritons, and alpha particles. No comparison could be made for the deuterons without introducing major changes in the output routines of the diffusion code.

The second step, charged-particle transport, could not be carried out with MCNP, so the neutron spectra

*Composed of 95.64% ^{6}Li, 4.36% ^{7}Li, and 99.9% D (at. %).

calculated here do not include this effect. Although the spectral changes are expected to be small with an external 14-MeV source, as employed in this experiment, this may not be the case for an operational fusion reactor.

II. EXPERIMENT

The experiment is well described in Ref. 1 and the reader is referred to that report for specific details. The primary purpose was to measure the tritium produced by neutrons interacting with ^{6}Li and ^{7}Li when the source spectrum is modified by traversing various thicknesses of ^{6}LiD. Figure 1 shows the geometry of the bottom half of the assembly. Ten hemishells of ^{6}LiD were machined and concentrically stacked with ampules of lithium hydride and radioactivation detectors placed at various positions along the radii. The inside radius, including the source and evacuated chamber, was 2.22 cm and the outside radius was 30.00 cm. In tabulation of the number of charged particles and neutrons produced, all sample masses were ignored since their combined masses were extremely small compared to the total mass of the ^{6}LiD sphere, which was 83.826 kg. The number of 14-MeV source neutrons that escaped from this assembly without colliding was relatively small (~3%). The total number of neutrons from the source was $9.42 \pm 0.28 \times 10^{15}$. The neutron flux distributions were measured by use of fission counters and a liquid scintillation detector (see Ref. 1).

III. PREDICTION OF THE NEUTRON SPECTRA AND CHARGED-PARTICLE PRODUCTION

Of the light charged particles (Z = 1, and 2), only ^{3}He is not abundantly produced from the interaction of neutrons with D and ^{6}Li. MCNP was used to calculate the protons, deuterons, tritons, and ^{4}He particles* produced from neutron interactions at 12 spherical surfaces along the ^{6}LiD radii. The experiment was mocked up in one dimension (using actual source flux and energy distributions[1]). Although the charged particles are not transported in MCNP, the neutrons, including those born in the ^{6}LiD, were followed throughout the system.

With the evaluated libraries for neutrons interacting with D (MAT = 120, ZAID = 1002.55), ^{6}Li (MAT = 1303, ZAID = 3006.50), and ^{7}Li (MAT = 3007, ZAID = 3007.55),** the charged particles produced from incident neutron reactions[2†] were easily tabulated from MCNP surface tallies at the several positions along the sphere radius. With the MCNP collision routines, 10,000 to 50,000 histories†† in a run produced aceptable statistics. A typical input file is given in Appendix A. The following reactions were considered:

1.	n + D → elastic scattering	(deuteron ions produced)
2.	n + D → n + n + p	(proton ions produced)
3.	n + D → γ + t	(insignificant since cross section is very small)
4.	n + ^{6}Li → t + α	(both tritons and alphas produced)
5.	n + ^{6}Li → p + ^{6}He	(ground state, which β^- decays to ^{6}Li; protons produced)
6.	n + ^{6}Li → n′ + d + α	(both deuterons and alphas produced)
7.	n + ^{6}Li → n′ + ^{6}Li	(2nd state, which γ decays to ground)
8.	n + ^{6}Li → 2n + p + α	(both protons and alphas produced)
9.	n + ^{7}Li → d + ^{6}He	(ground state deuterons produced)
10.	n + ^{7}Li → n′ + t + α	(both tritons and alphas produced)

*Although ^{6}Li ions are produced in large numbers from elastic scattering of neutrons, it has been assumed that these heavy ions slow down rather than undergo further interactions; therefore, they have not been tabulated here.

**R. C. Little,/X6CODE/XSLIST, Table 1 - Cross Sections maintained by X-6, (February 17, 1983). The ^{6}Li data are from ENDF/B-V; both the D and ^{7}Li are revised evaluations from Group T-2 at Los Alamos.

†The special MT numbers (reaction indices) available in MCNP were used to calculate the gas production (H,D, T, and ^{4}He) in this analysis.

††For the calculation of the neutron spectra, 100,000 histories were used to improve statistics in the spectral representations, which were expecially important below 1 MeV.

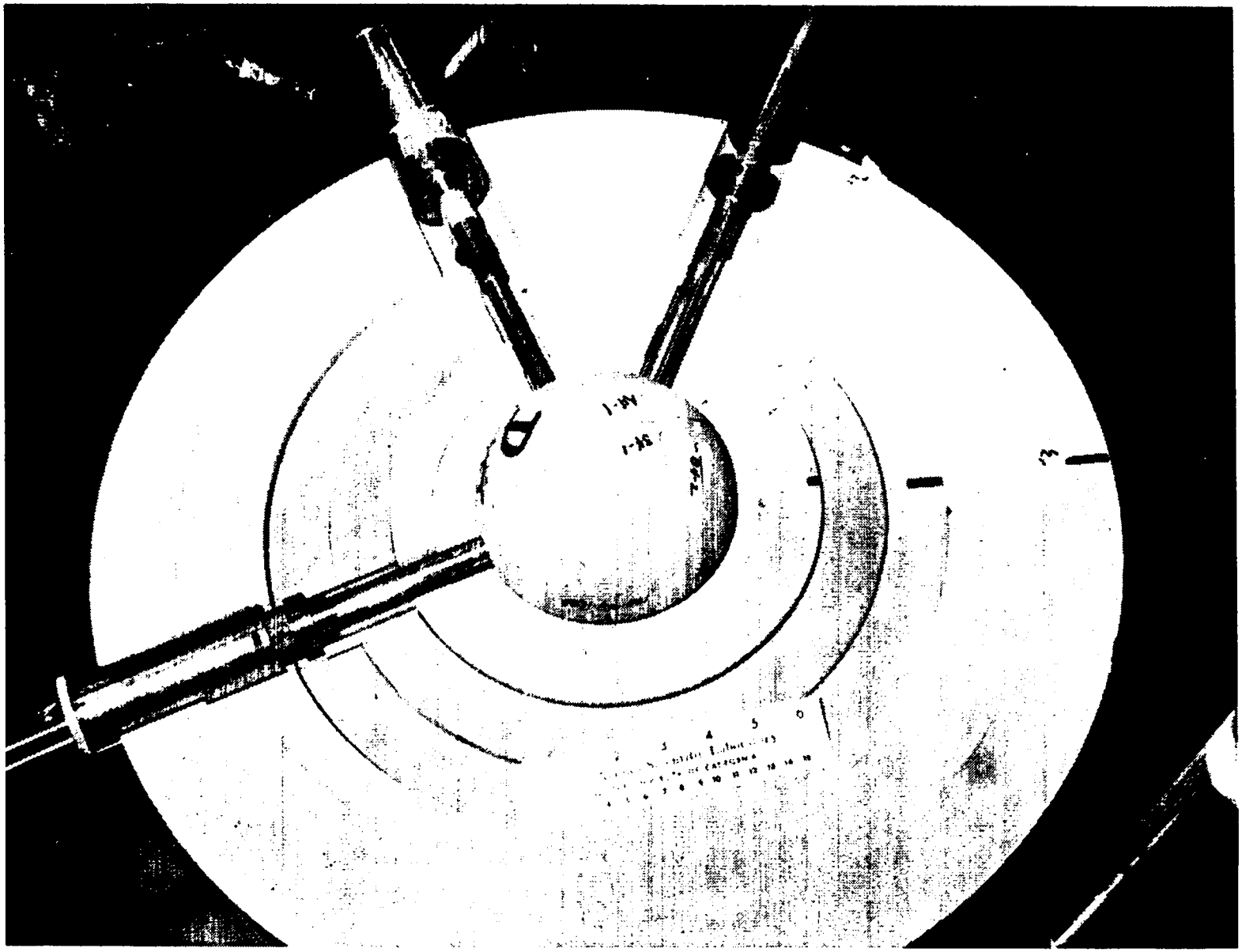

Fig. 1. Shells of ^{6}LiD mounted around the tritium target of the C-W machine. The bottom half of the assembly is complete; the outer top three hemishells are missing. This figure was taken from Ref. 1.

Note that all neutron interactions with ^{7}Li were included in the runs although the 4.4% abundance of ^{7}Li limited the charged particles produced to insignificant amounts, except for reactions 9 and 10 listed above.

The neutron spectra were tabulated at the same radial positions. The neutrons were transported through the ^{6}LiD, taking account of the 4.4% isotopic abundance of ^{7}Li. The lithium hydride ampules used to analyze the tritium production were assumed to contribute negligible mass and were ignored in the transport calculation.

IV. RESULTS

A. MCNP Charged-Particle Production

In the one-dimensional MCNP calculation, surface rather than "point" detectors were chosen for the experimental mockup to improve statistics for the same running times. The particle density (particles/cm^3) was then tabulated for each species (proton, deuteron, triton, and alpha particle) at 12 radial positions. To test the sensitivities of the different reactions, the data for each region were tabulated separately. A separate tabulation was also made for each important reaction that could provide some information on the maximum and minimum energies allowed for each of the charged particles omitted.

Of the charged particles produced when 14-MeV neutrons interact with ^{6}LiD, deuterons, which come mainly from elastic scattering, are by far the most prolific. When integrated over the sphere volume, 4.6 deuterons are produced per source neutron; the ratio is 1.4 for alphas, 0.8 for tritons, and 0.26 for protons. The numbers of particles produced as a function of radial position are also of interest; these are presented in Table I. These data were obtained in the following manner. The charged particle density, ρ (particles/cm^3), at surface i was averaged with the particle density at surface i + 1 to give an estimate of the average density of charged particles produced in the distance Δr. Then the average particle density times the volume between surfaces i and i + 1, when summed over the sphere, approximates the total number of particles produced in the ^{6}LiD sphere. For example, for a specific particle and reaction, the arithmetic expression:

$$N = \sum_{i=1}^{11} \frac{(\rho_i + \rho_{i+1})}{2} \times \frac{4\pi}{3} (r^3_{i+1} - r^3_i) \qquad (1)$$

has been used to estimate the number of charged particles produced. It is recognized that a linear average of the number of particles is not appropriate for all radii because the incident 14-MeV flux decreases as r^2 and the volume segment increases as r^3. The estimates presented in Table I are considered reasonable, however. More rigorous reaction rate calculations with MCNP indicate that the volume-integrated number of neutron-induced charged particles calculated using Eq. (1) may be approximately 3-5% high.

B. Comparison of the Tritium Production with Experiment

As mentioned previously, the tritium production was measured at several radial positions (5.00, 7.62, 12.6, 20.00, and 30.00 cm) by tritium recovery from ampules of lithium hydride embedded in the sphere of ^{6}LiD (see Ref. 1). An approximate comparison can be made using the densities calculated here. For ^{7}Li, the experimental values of tritium produced exceed the calculated values by an average of 3%. For ^{6}Li, the experimental values exceed the calculated values by an average of 20%. Thus, the calculated values of tritium produced are somewhat low, especially for ^{6}Li.

Precise comparison of the calculations with measurements in the lithium hydride ampules would necessitate a detailed mockup of the ampules themselves, which was not included in this analysis. This is particularly true for ^{6}LiH because of the large cross section for neutrons elastically scattered by hydrogen and because of the resonance in the ^{6}Li(n,t)α reaction. The detailed neutron flux distributions could be changed significantly by replacing the deuterium by hydrogen, expecially below 1 MeV, where the neutron scattering cross section of hydrogen is much larger. A calculation with lithium hydride in the ampules has been described by one of the authors.[3]

C. Charged-Particle Code Comparison

A comparison with the above calculations was made with a multigroup, neutron and charged-particle diffusion code which, in addition to tallying the charged particles produced by neutron reactions, follows the in-flight reactions among many of the charged particles themselves. The following reactions are included in this code:

$$\begin{aligned}
&d + D \rightarrow n + {}^3He + 3.269\ MeV\\
&d + D \rightarrow p + T + 4.034\ MeV\\
&d + T \rightarrow n + \alpha + 17.590\ MeV\\
&d + {}^3He \rightarrow p + \alpha + 18.354\ MeV\\
&d + {}^6Li \rightarrow n + {}^7Be + 3.382\ MeV\\
&d + {}^6Li \rightarrow p + {}^7Li + 5.027\ MeV\\
&d + {}^6Li \rightarrow p + T + \alpha + 2.558\ MeV\\
&d + {}^6Li \rightarrow \alpha + \alpha + 22.374\ MeV\\
&p + T \rightarrow n + {}^3He - 0.764\ MeV
\end{aligned}$$

TABLE I. Charged Particles Produced from 14-MeV Neutrons on ^{6}LiD

		Radial Position in the ^{6}LiD Sphere											
Position (cm):		2.23	3.00	4.00	5.00	6.00	7.62	10.00	12.60	16.00	20.00	24.00	30.00
Shell Volume (dV in cm^3):		66.6	155	256	381	949	2338	4190	8781	16,350	24,400	55,190	
PROTONS from D(n,2n)p	#/(D atom) × 10^{-13}	273	149	81.3	50.3	33.8	19.6	10.5	5.78	3.03	1.58	0.864	0.374
	#/cm^3 × 10^{10}	150	82.1	44.8	27.7	18.6	10.8	5.79	3.18	1.67	0.871	0.476	0.206
TOTAL PROTONS = 16.5 × 10^{14}		0.773	0.984	0.929	0.884	1.39	1.94	1.88	2.13	2.08	1.64	1.88	
PROTONS from ^{6}Li(n,p)All[a]	#/(^{6}Li atom) × 10^{-13}	128	70.3	38.9	24.1	16.3	9.56	5.17	2.88	1.53	0.808	0.446	0.192
	#/cm^3 × 10^{10}	67.5	37.0	20.5	12.7	8.59	5.04	2.72	1.52	0.806	0.425	0.235	0.101
TOTAL PROTONS = 7.84 × 10^{14}		0.348	0.446	0.425	0.404	0.645	0.927	0.889	1.02	1.01	0.805	0.928	
DEUTERONS from D(n,n)D	#/(D atom) × 10^{-13}	1402	1014	710	546	445	307	222	148	96.1	60.3	34.0	9.74
	#/cm^3 × 10^{10}	773	559	391	301	245	169	122	81.5	53.0	33.2	18.7	5.37
TOTAL DEUTERONS = 387 × 10^{14}		4.43	7.20	8.86	10.4	19.6	34.1	42.8	59.1	70.5	63.4	66.3	
DEUTERONS from ^{6}Li(n,n'd)α	#/(^{6}Li atom) × 10^{-13}	580	334	197	127	89.2	55.1	32.0	18.7	10.6	5.86	3.37	1.44
	#/cm^3 × 10^{10}	306	176	104	66.9	47.0	29.0	16.9	9.85	5.59	3.09	1.78	0.579
TOTAL DEUTERONS = 49.1 × 10^{14}		1.61	2.17	2.19	2.17	3.59	5.38	5.62	6.77	7.10	5.95	6.51	
TRITONS from ^{6}Li(n,t)α	#/(^{6}Li atom) × 10^{-13}	133	115	99.0	83.4	72.3	58.1	43.4	31.4	21.0	12.7	7.25	1.64
	#/cm^3 × 10^{10}	70.1	60.6	52.1	44.0	38.1	30.6	22.9	16.5	11.1	6.69	3.82	0.864
TOTAL TRITONS = 74.4 × 10^{14}		0.436	0.874	1.23	1.57	3.25	6.27	8.26	12.1	14.6	12.9	12.9	
TRITONS from ^{7}Li(n,n't)α	#/(^{7}Li atom) × 10^{-13}	463	258	146	91.8	63.3	37.8	21.1	12.0	6.57	3.56	2.00	0.883
	#/cm^3 × 10^{10}	11.1	6.19	3.50	2.20	1.52	0.907	0.506	0.288	0.158	0.085	0.048	0.021
TOTAL TRITONS = 1.47 × 10^{14}		0.058	0.075	0.073	0.071	0.115	0.165	0.167	0.196	0.198	0.163	0.193	
ALPHAS[b] from ^{6}Li(n,α)All[a]	#/(^{6}Li atom) × 10^{-13}	847	525	324	232	177	121	77.9	52.2	32.2	19.3	10.9	3.17
	#/cm^3 × 10^{10}	446	277	171	122	93.3	63.8	41.1	27.5	17.0	10.2	5.74	1.67
TOTAL ALPHAS = 130 × 10^{14}		2.41	3.47	3.76	4.11	7.44	12.3	14.4	19.6	22.3	19.5	20.5	

NOTE: The exponents in Column 2 should be multiplied by each number in each column which follows on that line. The source neutrons are 9.42 × 10^{15}.

[a] "All" indicates that more than one reaction is known to make a significant contribution to the tally.

[b] The total number of alpha particles from ^{7}Li is quite small and is therefore estimated from the ^{7}Li(n,n't) reaction listed above.

Note that the d + ^{6}Li → n + ^{3}He + α reaction, which has a positive Q of 1.80 MeV and is known to have a large cross section at low deuteron energies, has not yet been included in the code. In addition, elastic scattering of the charged particles among themselves is included only for Z = 1 and Z = 2.

The total protons, tritons, and α-particles produced are compared with MCNP results in Table II.

These results are considered in good agreement. The differences noted above are probably due to the different cross sections used in the two codes and to different algorithms in addition to statistical fluctuations.

More importantly, however, the diffusion code results do not indicate a large (or even perceptible, within the errors) number of charged particles produced by the

TABLE II. COMPARISON OF NUMBER OF PARTICLES PRODUCED

	Protons	Tritons	α-Particles
Diffusion	2.14×10^{15}	8.34×10^{15}	1.43×10^{16}
MCNP	2.43×10^{15}	7.59×10^{15}	1.31×10^{16}

secondary reactions. In the MCNP results, the neutron-induced reactions also produced many deuterons. A deuteron tally was not available in the diffusion code because the number of deuterium atoms in the LiD sphere far outweighed any buildup of deuterium.

D. Calculated Neutron Energy Spectra as a Function of Position in the ^{6}LiD Sphere

In the previous analysis (Ref. 1), the production of tritium from the ^{6}LiH and ^{7}LiH ampules and the activation of radiochemical detectors were calculated and compared with experimental data. Because both the lithium ampules and the activation detectors were placed at radial positions in the ^{6}LiD sphere considered in this analysis, the neutron energy spectra have been calculated at these as well as other radii. Figure 2 gives the neutron spectra below 1.0 MeV for the four positions closest to the neutron source, and Fig. 3 shows the data for four positions that represent deeper penetration in the sphere. Note the flux depression near 250 keV is apparent at all positions from the resonance in the ^{6}Li(n,t)α reaction.

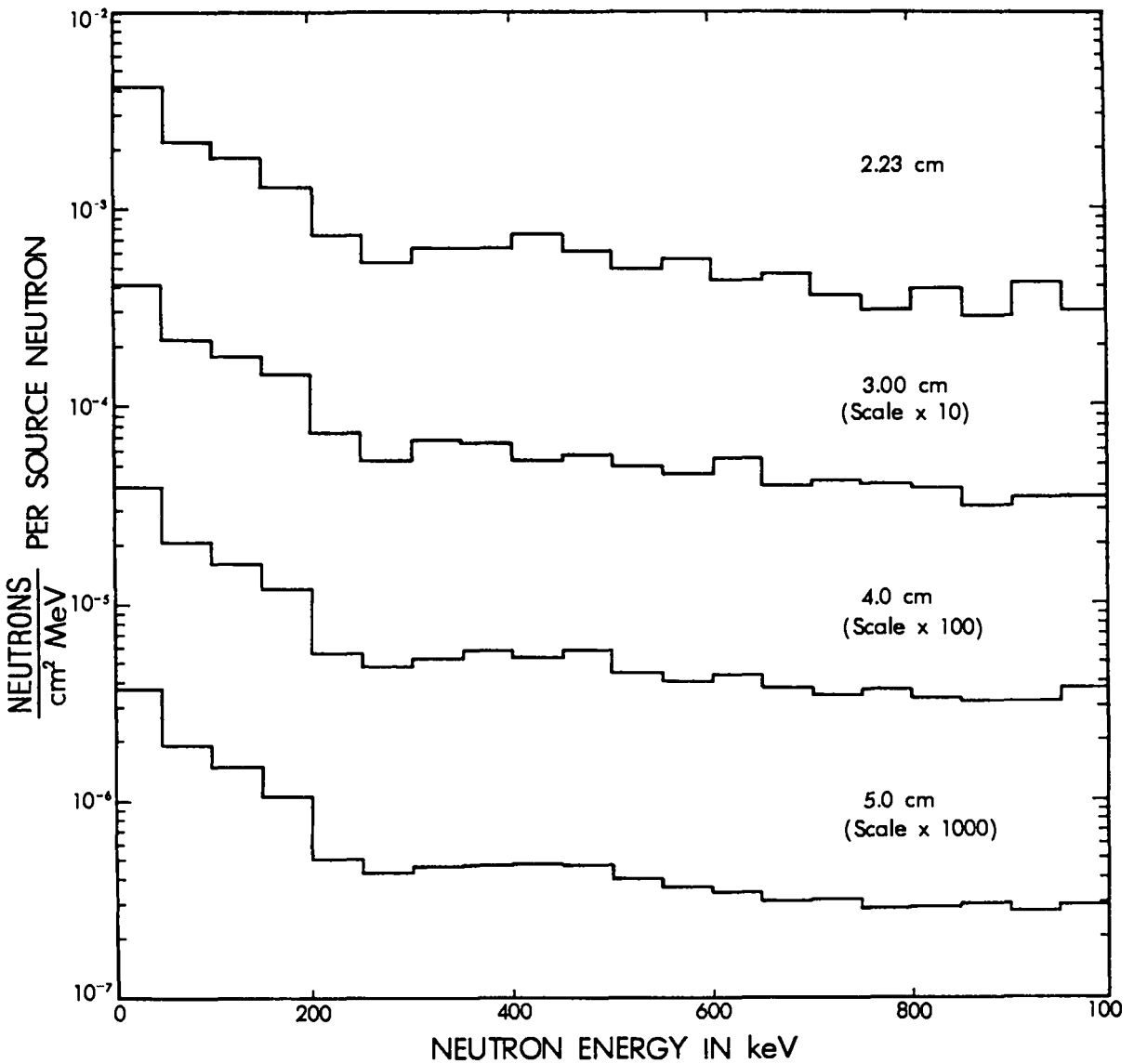

Fig. 2. Neutrons cm^{-2} MeV^{-1} per source neutron as a function of radial position for neutrons below 1.0 MeV. The four positions closest to the source are shown here.

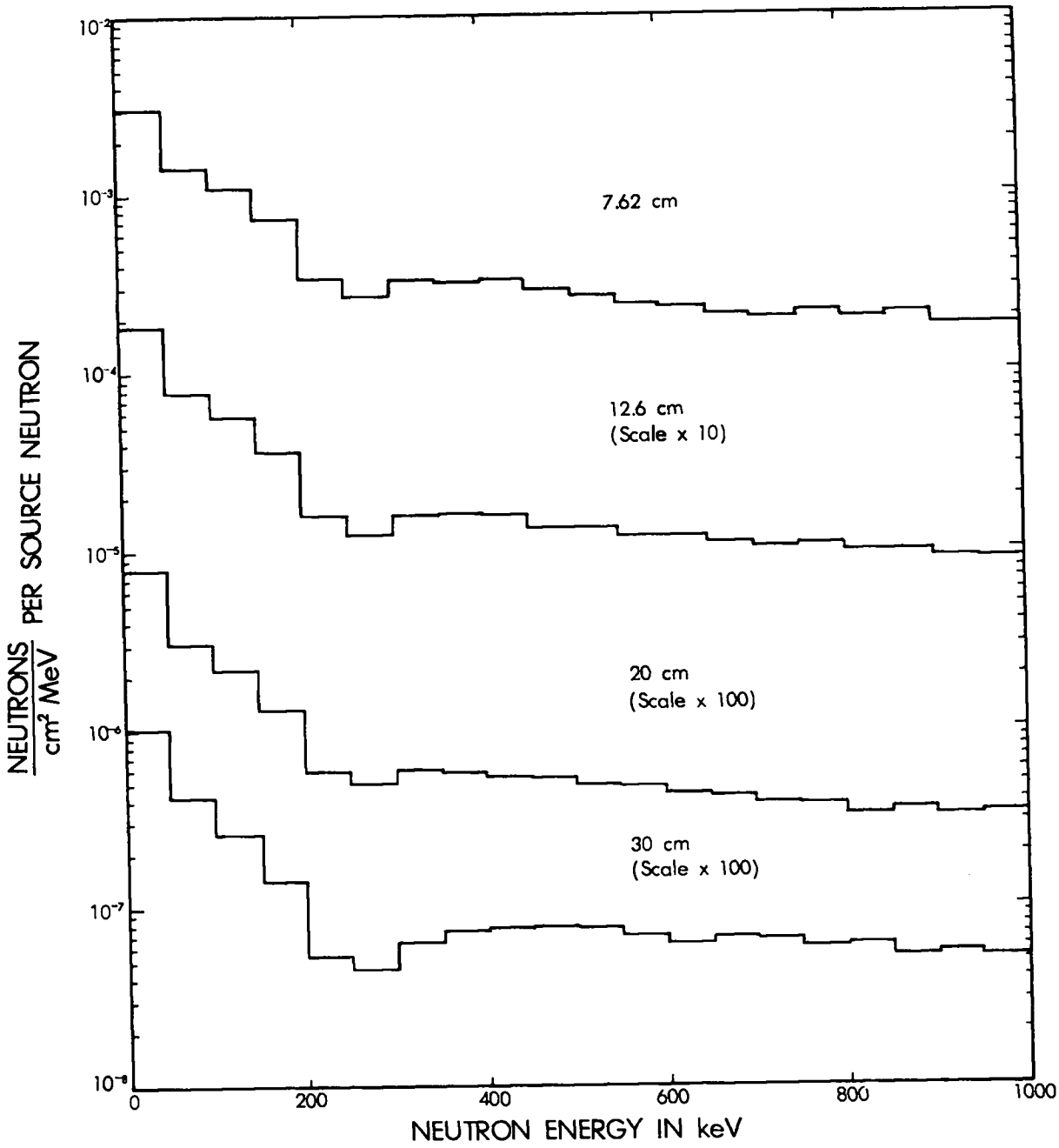

Fig. 3. Neutrons cm^{-2} MeV^{-1} per source neutron as a function of radial position for neutrons below 1.0 MeV. Four positions chosen far from the source are shown here.

Figure 4 shows the spectra over the entire energy range for three positions near the source and Figure 5 shows similar data at three positions far from the source. No structure is seen at high energy although the rapid degradation of the source neutrons with deeper penetration is apparent. Table III contains all the neutron spectra in tabular form for the 12 radial positions, where, for convenience, they have been normalized to one source neutron. A most interesting point is found in comparing the tritons produced in Table I at radial positions of 2.23 and 20 cm. Although the incident neutron flux is expected to decrease by a

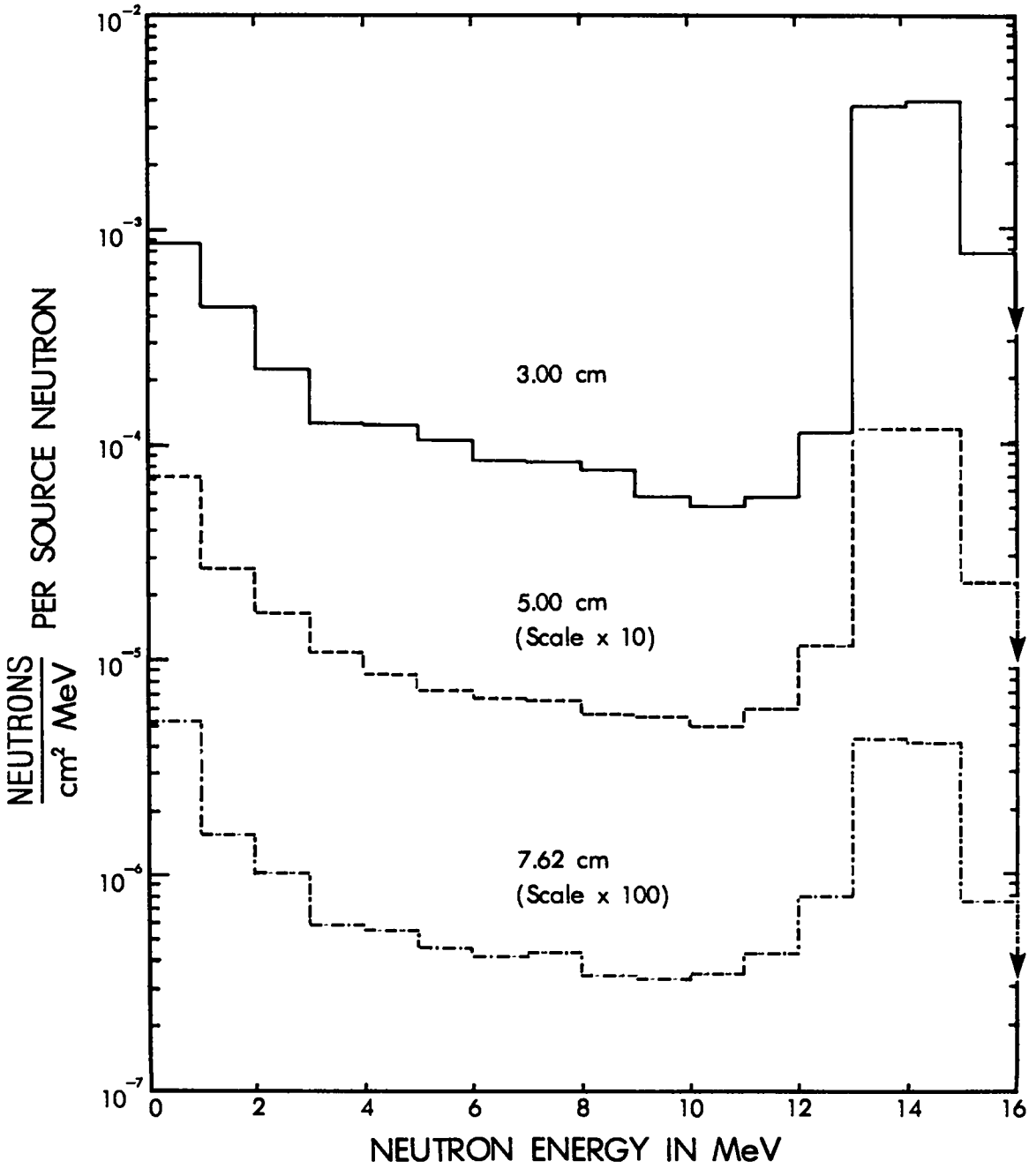

Fig. 4. Neutrons cm^{-2} MeV^{-1} per source neutron as a function of radial position for neutrons of all energies. Three positions chosen close to the neutron source are shown here.

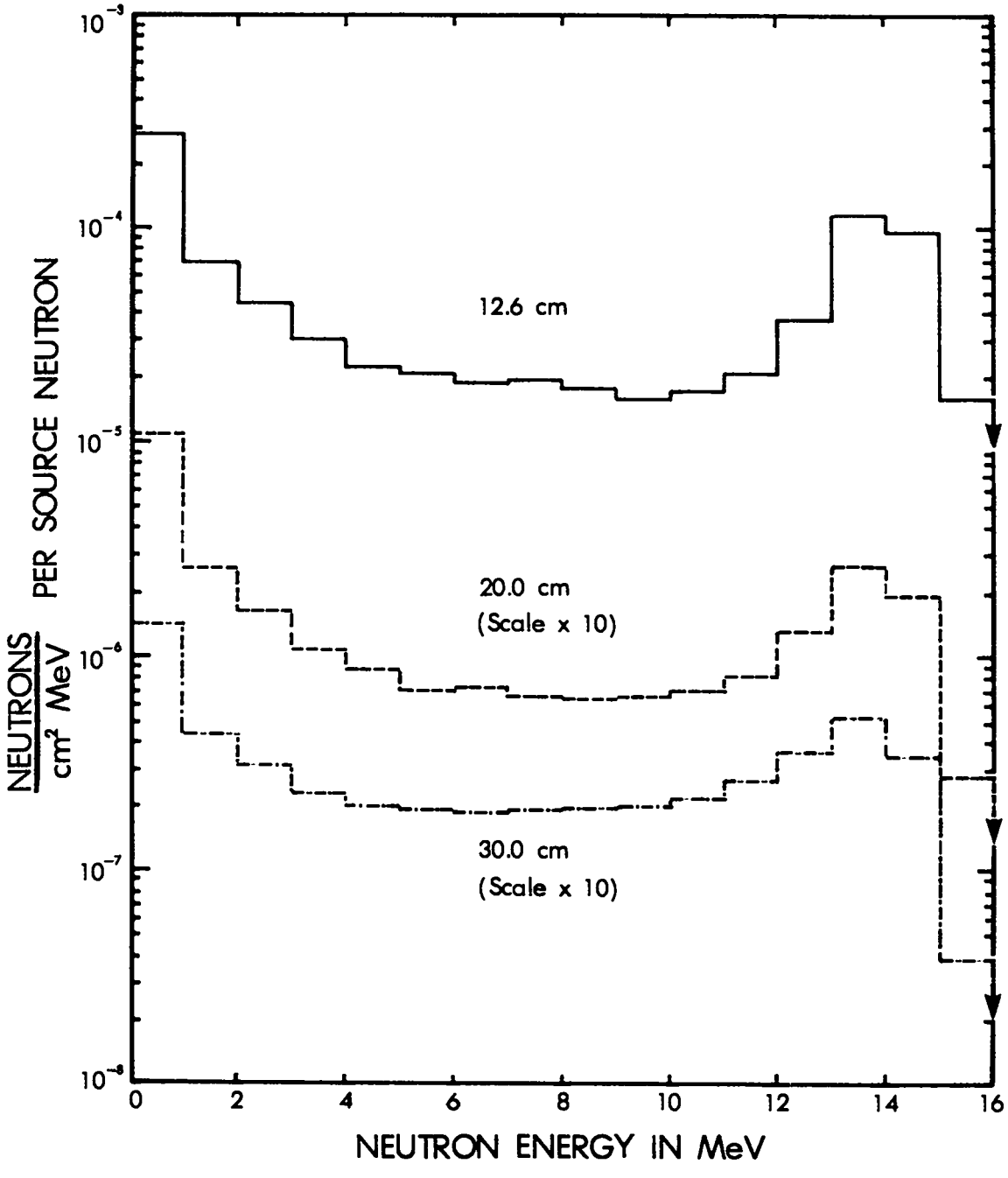

Fig. 5. Neutrons cm^{-2} MeV^{-1} per source neutron as a function of radial position for neutrons of all energies. Three positions far from the neutron source are shown here.

TABLE III. The Neutron Spectrum (Neutrons/cm^2 MeV^{-1} per Source Neutron) as a Function of Radial Distance from the Source

E_n (MeV) \ Radial Position (cm)	2.23	3.00	4.00	5.00	6.00	7.62	10.00	12.60	16.00	20.00	24.00	30.00
0.05[a]	4.197-3[b]	4.083-3	3.938-3	3.751-3	3.463-3	3.038-3	2.437-3	1.840-3	1.278-3	8.014-4	4.622-4	1.024-4
0.10	2.190-3	2.222-3	2.088-3	1.926-3	1.696-3	1.425-3	1.076-3	7.831-4	5.044-4	3.120-4	1.838-4	4.244-5
0.15	1.842-3	1.818-3	1.613-3	1.506-3	1.271-3	1.085-3	7.935-4	5.756-4	3.577-4	2.206-4	1.267-4	2.589-5
0.20	1.268-3	1.438-3	1.221-3	1.047-3	9.358-4	7.349-4	5.142-4	3.626-4	2.186-4	1.311-4	7.592-5	1.430-5
0.25	7.451-4	7.484-4	5.696-4	5.070-4	4.506-4	3.418-4	2.412-4	1.611-4	9.880-5	5.919-5	3.427-5	5.392-6
0.30	5.418-4	5.294-4	4.879-4	4.356-4	3.481-4	2.686-4	1.881-4	1.234-4	7.931-5	5.067-5	2.581-5	4.489-6
0.35	6.553-4	6.779-4	5.269-4	4.692-4	3.989-4	3.326-4	2.278-4	1.603-4	9.945-5	5.944-5	3.269-5	6.430-6
0.40	6.520-4	6.507-4	5.846-4	4.756-4	3.975-4	3.180-4	2.158-4	1.633-4	9.886-5	5.797-5	3.355-5	7.342-6
0.45	7.617-4	5.425-4	5.487-4	4.809-4	3.960-4	3.333-4	2.299-4	1.587-4	9.703-5	5.518-5	3.181-5	7.683-6
0.50	6.196-4	5.794-4	5.887-4	4.764-4	3.947-4	2.906-4	2.208-4	1.361-4	8.678-5	5.404-5	3.184-5	7.782-6
0.55	4.982-4	5.051-4	4.563-4	4.070-4	3.440-4	2.707-4	1.869-4	1.364-4	8.273-5	4.887-5	2.887-5	7.667-6
0.60	5.708-4	4.570-4	4.101-4	3.697-4	3.194-4	2.421-4	1.808-4	1.211-4	7.705-5	4.843-5	2.682-5	6.890-6
0.65	4.440-4	5.571-4	4.420-4	3.535-4	2.883-4	2.327-4	1.600-4	1.189-4	7.914-5	4.409-5	2.606-5	6.186-6
0.70	4.866-4	4.046-4	3.797-4	3.149-4	2.686-4	2.131-4	1.533-4	1.123-4	6.396-5	4.150-5	2.473-5	6.775-6
0.75	3.740-4	4.256-4	3.516-4	3.216-4	2.768-4	2.013-4	1.362-4	1.034-4	6.923-5	3.904-5	2.531-5	6.620-6
0.80	3.162-4	4.124-4	3.741-4	2.906-4	2.625-4	2.164-4	1.433-4	1.068-4	6.225-5	3.831-5	2.191-5	5.861-6
0.85	4.068-4	3.960-4	3.391-4	2.964-4	2.686-4	1.974-4	1.368-4	9.896-5	5.857-5	3.360-5	2.031-5	6.154-6
0.90	2.934-4	3.374-4	3.283-4	3.051-4	2.407-4	2.132-4	1.382-4	9.898-5	6.156-5	3.563-5	2.111-5	5.243-6
0.95	4.344-4	3.621-4	3.296-4	2.793-4	2.197-4	1.817-4	1.443-4	9.246-5	5.844-5	3.220-5	1.779-5	5.557-6
1.00	3.153-4	3.649-4	3.848-4	3.013-4	2.399-4	1.817-4	1.214-4	8.921-5	5.423-5	3.348-5	1.880-5	5.196-6
2.00	4.790-4	4.442-4	3.338-4	2.685-4	2.208-4	1.546-4	1.034-4	6.911-5	4.389-5	2.602-5	1.536-5	4.460-6
3.00	2.236-4	2.275-4	1.961-4	1.650-4	1.291-4	1.033-4	6.472-5	4.410-5	2.650-5	1.663-5	9.700-6	3.177-6
4.00	8.578-5	1.257-4	1.181-4	1.088-4	8.745-5	5.813-5	4.475-5	2.968-5	1.770-5	1.110-5	6.511-6	2.341-6
5.00	6.714-5	1.220-4	9.364-5	8.617-5	6.503-5	5.471-5	3.490-5	2.241-5	1.455-5	8.796-6	4.808-6	2.036-6
6.00	7.567-5	1.019-4	9.336-5	7.290-5	6.091-5	4.523-5	3.219-5	2.078-5	1.358-5	7.096-6	4.877-6	1.964-6
7.00	7.314-5	8.724-5	7.384-5	6.705-5	5.731-5	4.196-5	2.754-5	1.882-5	1.260-5	7.254-6	4.417-6	1.917-6
8.00	7.180-5	8.570-5	7.384-5	6.549-5	5.280-5	4.272-5	2.877-5	1.957-5	1.175-5	6.598-6	4.025-6	1.952-6
9.00	3.415-5	7.647-5	7.318-5	5.711-5	4.679-5	3.390-5	2.490-5	1.782-5	1.150-5	6.399-6	4.021-6	2.021-6
10.00	3.199-6	5.848-5	5.671-5	5.545-5	4.682-5	3.327-5	2.382-5	1.627-5	1.118-5	6.613-6	4.092-6	2.036-6
11.00	1.751-6	5.321-5	5.414-5	5.008-5	4.359-5	3.484-5	2.544-5	1.759-5	1.145-5	7.065-6	4.358-6	2.233-6
12.00	0.0	5.671-5	6.570-5	6.061-5	5.380-5	4.247-5	2.950-5	2.075-5	1.313-5	8.254-6	5.353-6	2.720-6
13.00	0.0	1.129-4	1.353-4	1.178-4	1.038-4	7.923-5	5.481-5	3.728-5	2.269-5	1.318-5	7.856-6	3.705-6
14.00	6.990-3	3.699-3	1.964-3	1.183-3	7.699-4	4.331-4	2.182-4	1.135-4	5.517-5	2.635-5	1.344-5	5.228-6
15.00	7.467-3	3.885-3	2.016-3	1.189-3	7.590-4	4.119-4	1.911-4	9.571-5	4.381-5	1.954-5	9.359-6	3.501-6
16.00	1.545-3	7.863-4	3.973-4	2.299-4	1.436-4	7.466-5	3.400-5	1.584-5	6.742-6	2.792-6	1.245-6	3.888-7
Neutrons/cm^2	1.70+14[c]	1.02+14	6.16+13	4.23+13	3.07+13	2.03+13	1.24+13	7.87+12	4.67+12	2.67+12	1.53+12	5.11+11

[a] This energy represents the upper limit of the bin.

[b] Read as 4.197×10^{-3} neutrons/cm^2 MeV^{-1} per source neutron. The last significant figure is not meaningful but is carried here as a check for small arithmetic errors.

[c] The number of neutrons/cm^2, after integrating the above spectrum over energy and multiplying by the number of source neutrons (9.42×10^{15}).

factor of approximately 80 because of the increase in r^2, the number of tritons produced decreased by little more than a factor of 10. This difference is reflected in the energy dependence of the (n,t) cross section, which is smallest near 14 MeV (~25 mb) and rises steeply as the neutron energy decreases.

E. Calculated Neutron Current Distributions Using MCNP

In parts A, B, and D of this section, results have been presented based on MCNP calculations of neutron flux (more correctly, neutron fluence). Here we summarize results of MCNP calculations of the neutron current. The current as calculated in MCNP for this problem is defined to be the total neutrons crossing a surface (there is no calculation of "net" current). Table IV indicates the calculated neutron current at various locations within the ^{6}LiD assembly. All results in Table IV have a statistical uncertainity $\leq 1.2\%$. The current (in units of number of neutrons per source neutron) increases with increasing radius from the source up to 10 cm and decreases from 10 to 30 cm. Time-integrated currents greater than 1.0 are caused by a neutron crossing the same tally surface more than once and also by (n,Xn) reactions. The neutron current as a function of energy has also been obtained at various locations. Selected spectral results are given in Table V and plotted in Figs. 6-8.

V. CONCLUSIONS

It has been shown that large fluxes of hydrogen and helium-4 ions are produced when 14-MeV neutrons

TABLE IV. Calculated Neutron Current as a Function of Position

Surface	Radius (cm)	Current (#/source neutron)
1	2.230	1.06
2	3.000	1.09
3	4.000	1.13
4	5.001	1.16
5	6.000	1.19
6	7.616	1.22
7	10.000	1.24
8	12.602	1.21
9	16.000	1.11
10	20.002	0.969
11	24.000	0.789
12	30.002	0.461

TABLE V. Neutron Current Spectrum (Neutrons/MeV per Source Neutron) as a Function of Radial Distance from the Source

E_n (MeV) \ Radial Position (cm)	3.00	10.00	24.00
0.001[a]	2.401 − 1[b]	2.499 + 0	2.815 + 0
0.005	4.097 − 1	2.975 + 0	3.588 + 0
0.01	3.478 − 1	2.412 + 0	2.730 + 0
0.05	1.998 − 1	1.288 + 0	1.400 + 0
0.1	1.154 − 1	6.934 − 1	7.295 − 1
0.5	5.118 − 2	2.113 − 1	1.821 − 1
1.0	2.412 − 2	9.784 − 2	8.928 − 2
2.0	2.731 − 2	7.624 − 2	5.978 − 2
3.0	1.251 − 2	5.302 − 2	3.796 − 2
4.0	7.042 − 3	3.375 − 2	2.981 − 2
5.0	7.612 − 3	2.730 − 2	2.387 − 2
6.0	6.567 − 3	2.819 − 2	2.331 − 2
7.0	5.485 − 3	2.559 − 2	2.207 − 2
8.0	5.369 − 3	2.337 − 2	1.799 − 2
9.0	4.038 − 3	2.140 − 2	2.288 − 2
10.0	3.962 − 3	2.452 − 2	2.350 − 2
11.0	3.862 − 3	2.629 − 2	2.562 − 2
12.0	5.198 − 3	3.192 − 2	3.409 − 2
13.0	1.186 − 2	6.504 − 2	5.078 − 2
14.0	4.215 − 1	2.739 − 1	9.638 − 2
15.0	4.330 − 1	2.374 − 1	6.936 − 2
20.0	1.766 − 2	9.091 − 3	2.094 − 3
TOTAL	1.030 + 16[c]	1.168 + 16	7.428 + 15

[a]This energy represents the upper limit of the bin.
[b]Read as 2.401×10^{-1} neutrons/MeV per source neutron.
[c]The total number of neutrons, after integrating the above spectrum over energy and multiplying by the number of source neutrons (9.42×10^{15}).

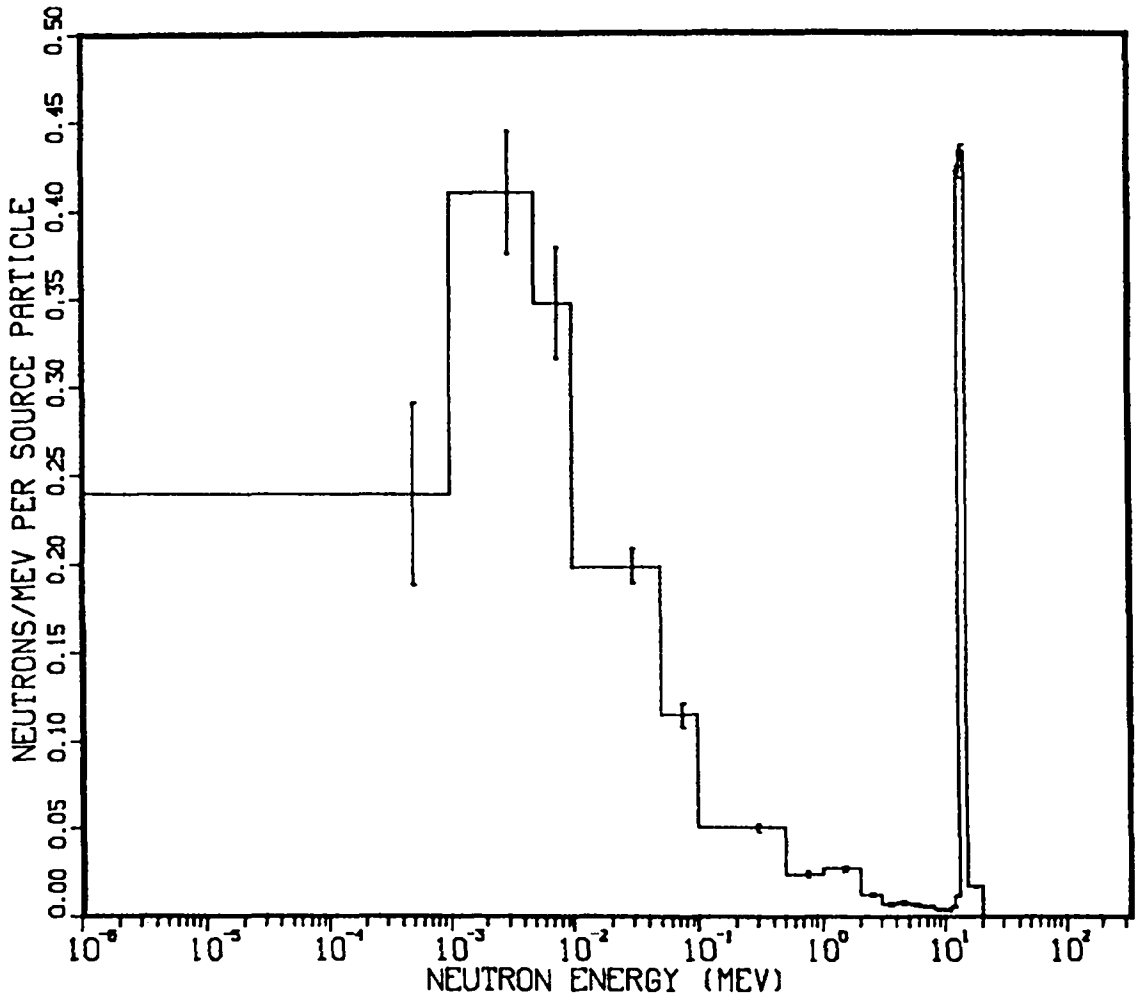

Fig. 6. Calculated neutron current at a radius of 3 cm.

interact with kilogram quantities of ^{6}LiD. Elastic scattering of neutrons by ^{6}Li would also produce a significant number of ^{6}Li ions, but these particles were not tallied in this MCNP analysis.

The energy spectra of these charged ions were not obtained although they would be necessary for charged-particle transport calculations. Currently, MCNP does not follow these particles. Many of the input data are not yet available in the ENDF system; these problems are discussed in more detail in Appendix B.

It is hoped that charged-particle transport in this ^{6}LiD system can be carried out at some future date. Even a rough estimate of the contributions from the ^{6}Li and ^{7}Li reactions to the source neutron spectra [d(d,n) and T(d,n)] would be both useful and interesting. If a significant fraction of the neutrons produced should appear near or above the 14-MeV peak, other programs could be affected, such as shielding. A further study is therefore recommended when the charged-particle production* and charged-particle transport data are reasonably well defined.

ACKNOWLEDGMENTS

The authors are grateful to Raymond Hunter, Robert Schrandt, Robert Seamon, Guy Estes, and Don Barr for their assistance, encouragement, and support. We would also like to especially thank Gary Corman and Robert Howerton of Lawrence Livermore National Laboratory for providing us with some of the charged-particle input data.

*This includes the energy and angular distributions of the charged particles produced from the neutron interactions..

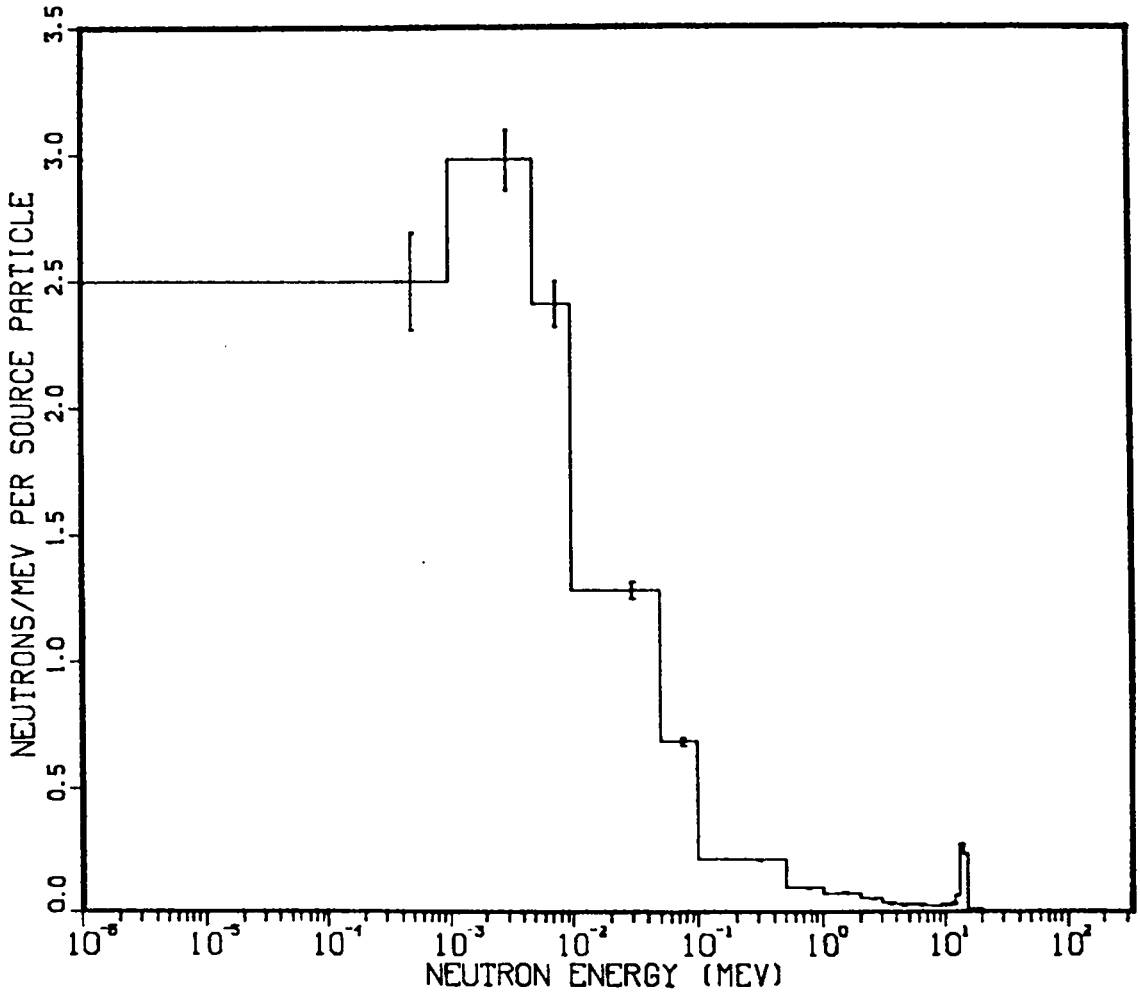

Fig. 7. Calculated neutron current at a radius of 10 cm.

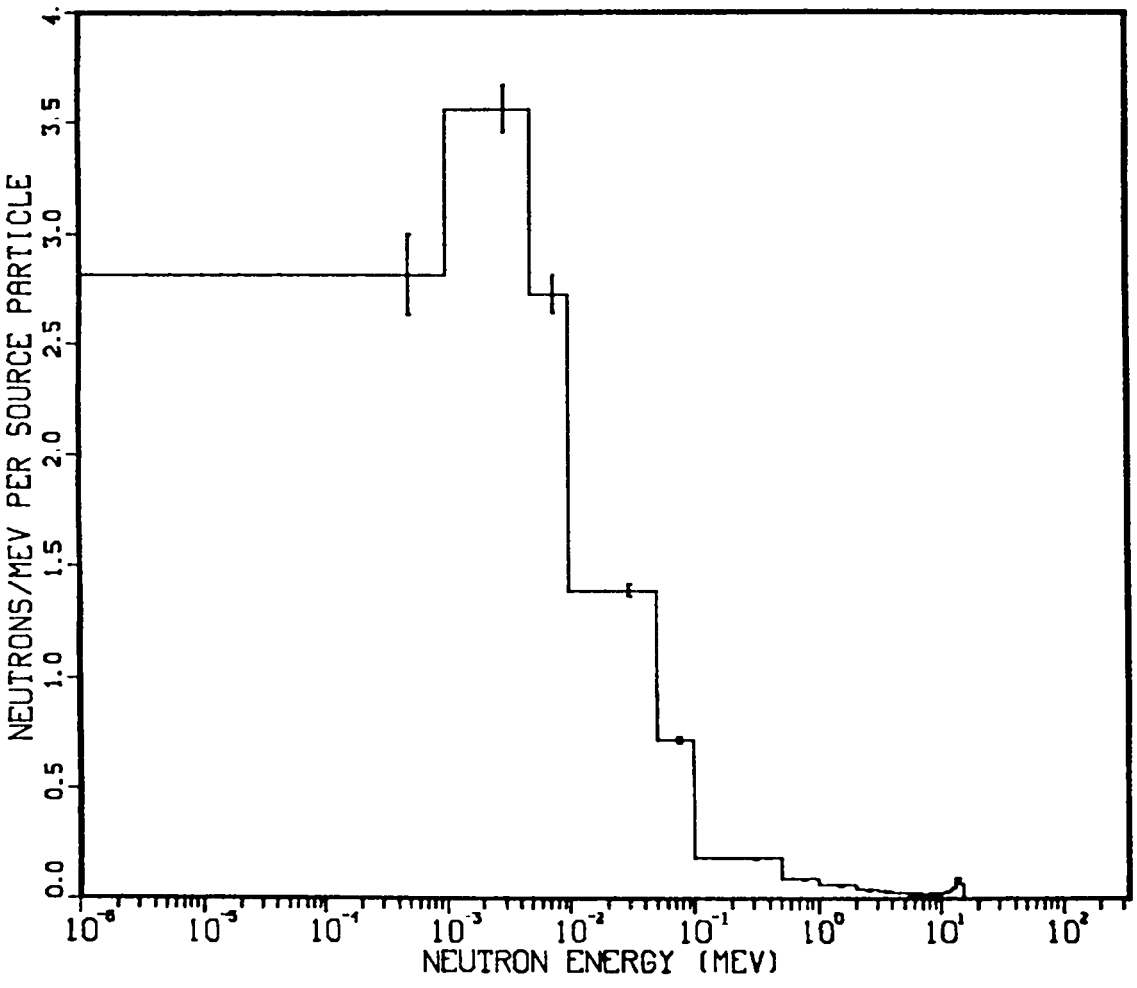

Fig. 8. Calculated neutron current at a radius of 24 cm.

REFERENCES

1. A. Hemmendinger, C. E. Ragan, E. R. Shunk, A. N. Ellis, J. M. Anaya, and Jon M. Wallace, "Tritium Production in a Sphere of ^{6}LiD Irradiated by 14-MeV Neutrons," Los Alamos Scientific Laboratory report LA-7310 (October 1978).

2. Los Alamos Monte Carlo Group, "MCNP—A General Monte Carlo Code for Neutron and Photon Transport," Los Alamos National Laboratory report LA-7396-M (Rev.) (April 1981).

3. L. R. Fawcett, Jr., "Reanalysis of Tritium Production in a Sphere of ^{6}LiD Irradiated by 14-MeV Neutrons," Los Alamos National Laboratory report LA-10506-MS (August 1985).

APPENDIX A

Sample Input for MCNP Runs

```
LiD Shells Surface Tally (Charged Particle Production)

 1     0                -1
 2     4     -0.689      1      - 2
 3     4     -0.689      2      - 3
 4     4     -0.689      3      - 4
 5     4     -0.708      4      - 5
 6     4     -0.708      5      - 6
 7     4     -0.734      6      - 7
 8     4     -0.734      7      - 8
 9     4     -0.739      8      - 9
10     4     -0.739      9      -10
11     4     -0.744     10      -11
12     4     -0.744     11      -12
21     0                12

 1     SO     2.230
 2     SO     3.000
 3     SO     4.000
 4     SO     5.001
 5     SO     6.000
 6     SO     7.616
 7     SO    10.000
 8     SO    12.602
 9     SO    16.000
10     SO    20.002
11     SO    24.000
12     SO    30.002

IN    2  2 2 2 2 2  1  1 1 1 1 2 0
SRC   0  1 0 0 0 0 100 0 0 0 0 0 0
FILES   14 BBSRC
EO     1-3 5-3 1-2 5-2 1-1 5-1 1 2 3 4 5 6 7 8 9 10 11 12 13 14 15 20
F2     1  2  3  4  5  6  7  8  9  10  11  12
FM2    0.942E-8  2  203
F22    1  2  3  4  5  6  7  8  9  10  11  12
FM22   0.942E-8  2  2
F42    1  2  3  4  5  6  7  8  9  10  11  12
FM42   0.942E-8  3  203
F62    1  2  3  4  5  6  7  8  9  10  11  12
FM62   0.942E-8  3  204
F82    1  2  3  4  5  6  7  8  9  10  11  12
FM82   0.942E-8  3  205
F102   1  2  3  4  5  6  7  8  9  10  11  12
M2      1002.55    1.
M3      3006.50    1.
M4      1002.55    0.5    3006.50    0.4782    3007.55    0.0218
NPS     100000
CTME 60
TOTNU
ERGN 0.    20.0
CUTN  1.0E123  1.0E-6  -0.1  -0.025
PRDMP  100000        100000
NSPLIT 4  1.0
```

APPENDIX B

Evaluated Data Needed in The ENDF System

The information needed in the ENDF system for charged-particle transport is enormous. Neutrons with energies up to 35 MeV can be produced when high-energy charged particles interact with lithium deuteride systems. The cross sections for the production of these charged particles via neutron interactions are required. In addition, the energy and angular distributions of charged particles are necessary. Extension of the neutron data above 20 MeV is also required.

Providing these evaluated files would be a major additional effort for the ENDF system. Many problems are already obvious: 1) no national program is in place for establishing such an evaluated library; 2) no national program is in place for compiling and distributing the experimental data for charged-particle interactions upon which the evaluations would be based; 3) the users are scattered and have different priorities; and 4) the character of the charged-particle data is so varied compared to neutrons incident that experiment, compilation, and evaluation programs are more difficult to bring under one umbrella.

Further elaboration on 4) should be extensive for sufficient comprehension. Only a few points will be made here. First, the Lawrence Livermore National Laboratory initiated its own program several years ago and this program continues. The LLNL staff is provided with computerized input evaluated data. Both incident neutron and charged-particle input data are complete enough to perform charged-particle transport calculations up to 20 MeV. That laboratory is unique in performing this function. By restricting their effort to a few reactions required by specific internal users, they have made tremendous strides in this direction. If a national effort is to be initiated, one could profit extensively from a study of the Livermore program. It is important to note that handling such a computerized file requires extensive retrieval, processing, checking, and plotting programs.

The character of the charged-particle interactions is a bit different from that of neutrons. First, charged-particle interactions are inhibited by the coulomb barrier. Second, large positive Q values obtain, especially when deuterons and tritons are the incident particles. For example, the T(d,n) reaction Q value is 17.59 MeV and the D(d,n) Q value is 3.269 MeV. These are the primary reactions considered for the first-generation fusion reactor, and they have been subjected to a variety of experimental studies, especially in the low-MeV range. Very little is known about the T(t,2n) cross section, however, even though the Q is 11.33 MeV and two neutrons and an alpha particle are produced.

For deuterons and tritons incident on ^{6}Li and ^{7}Li, many positive Q reactions have been observed with large intensities of neutrons, protons, deuterons, tritons, gamma rays, and radioactive products in the exit channel. Much information is required to calculate the "prompt" and "delayed" heating; neutron and proton production; and hydrogen and helium production. A further complication in evaluation is that sequential decay mechanisms often dominate the interaction probabilities. Target and fuel absorption or production could be important in certain applications.

For protons incident on ^{6}Li and ^{7}Li several reactions are important and a few have positive Q values. For example, the ^{7}Li(p,2α) reaction has a Q value of 17.35 MeV. Protons, deuterons, and tritons produced in Li often have energies above 10 MeV.

The experimental data base for these reactions is extremely sparse and imprecise. Most of the measurements are reported as relative values, and often these are not provided with sufficient information to enable absolute normalizations. Because charged particles emitted in many reactions can have energies up to 20 MeV or more, the energy dependence of the cross sections is required over large energy ranges. In addition, the neutrons emitted in charged-particle reactions can significantly exceed the maximum energy range of the neutron evaluated library of 20 MeV (ENDF/B).

As the fusion reactor concept matures, perhaps the need for expanding and improving the evaluated data files will be more apparent. Certainly, establishing priorities could limit the input necessary so that future studies can determine the importance of charged-particle transport.

Printed in the United States of America
Available from
National Technical Information Service
US Department of Commerce
5285 Port Royal Road
Springfield, VA 22161

Microfiche (A01)

Page Range	NTIS Price Code	Page Range	NTIS Price Code	Page Range	NTIS Price Code	Page Range	NTIS Price Code
001-025	A02	151-175	A08	301-325	A14	451-475	A20
026-050	A03	176-200	A09	326-350	A15	476-500	A21
051-075	A04	201-225	A10	351-375	A16	501-525	A22
076-100	A05	226-250	A11	376-400	A17	526-550	A23
101-125	A06	251-275	A12	401-425	A18	551-575	A24
126-150	A07	276-300	A13	426-450	A19	576-600	A25
						601-up*	A99

*Contact NTIS for a price quote.

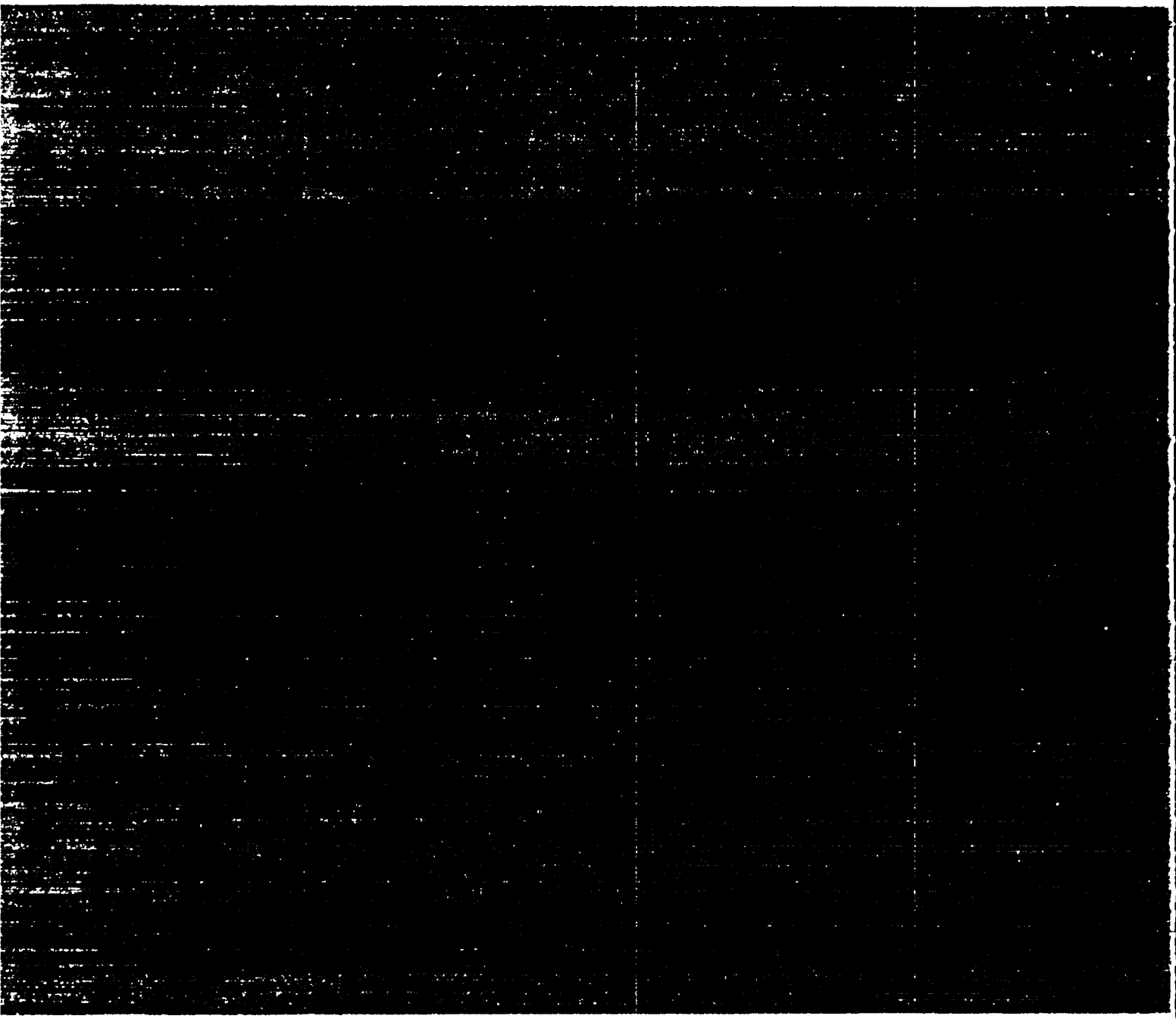

Los Alamos